

# Nanopatterning With Interferometric Lithography Using a Compact $\lambda = 46.9$ -nm Laser

Maria G. Capeluto, Georgiy Vaschenko, Michael Grisham, Mario C. Marconi, S. Ludueña, L. Pietrasanta, Yunfeng Lu, Bruce Parkinson, Carmen S. Menoni, *Senior Member, IEEE*, and J. J. Rocca

**Abstract**—We report the imprinting of nanometer-scale gratings by interferometric lithography at  $\lambda = 46.9$  nm using an Ne-like Ar capillary discharge laser. Gratings with periods as small as 55 nm were imprinted on poly-methyl methacrylate using a Lloyd's mirror interferometer. This first demonstration of nanopatterning using an extreme ultraviolet (EUV) laser illustrates the potential of compact EUV lasers in nanotechnology applications.

**Index Terms**—Nanotechnology, photolithography, X-ray lasers, X-ray lithography.

THE increasing activity in nanotechnology and nanoscience fuels the need to realize fabrics of periodic structures in the nanometer range. Along this path, table-top extreme ultraviolet (EUV) sources offer exciting new opportunities to demonstrate novel fabrication tools capable of reaching nanometer resolution in small laboratory environments. High repetition rate table-top EUV lasers provide a useful way to record nanoscale features, particularly when the pattern can be created by interference effects that take advantage of the coherence of this type of compact EUV sources. Such maskless scheme, known as interferometric lithography (IL), is capable of producing regular patterns of lines or dots with features approaching  $\lambda/2$  over large areas [1]–[6].

IL has been previously demonstrated with ultraviolet (UV) and vacuum-ultraviolet (VUV) laser light illumination at 157 nm [7], 193 nm [6], and 257 nm [8], and with 13-nm synchrotron radiation [2], [3]. With VUV lasers, sub-100-nm gratings and grids have been printed using different optical

schemes [7], [9]. With the shorter wavelength from the synchrotron source, 38-nm period gratings were imprinted in poly-methyl methacrylate (PMMA) [2]. Clearly, decreasing the wavelength provides a direct path to decreasing feature size. Obtaining a good quality interference pattern also requires the illumination source to have a high degree of coherence and high average power to allow for short exposure times. The high spatial and temporal coherence are also essential for large-area coverage, as will be discussed later in more detail. The capillary discharge lasers are the first compact EUV sources to achieve both relatively high average power and high spatial and temporal coherence [10], [11].

Herein, we report on the imprinting of nanometer-scale gratings using IL at  $\lambda = 46.9$  nm, implemented with a compact Ne-like Ar capillary discharge laser. The experiment takes advantage of the unique characteristics of this laser [10], [11] to print lines as small as 28-nm wide (55-nm period) in commercial-grade PMMA films using a single-mirror interferometer.

The capillary discharge laser used as the source of EUV radiation was configured to produce pulses with an energy of  $\sim 0.15$  mJ and a duration of  $\sim 1.2$ -ns full width at half maximum (FWHM). In this experiment, the laser used 27-cm-long plasma channels and was operated at a 1-Hz repetition rate. An increased average power, of up to a few milliwatts, could be obtained operating this source at a repetition rate of 4–10 Hz with longer capillaries, however, at the expense of reduced lifetime of the capillary tube [10]. At the capillary exit, the FWHM of the beam diameter varies from 150 to 300  $\mu\text{m}$  depending on the discharge conditions. In the far field, the beam has a characteristic annular shape, which is a consequence of refraction caused by the plasma density gradients in the capillary. Its cross section has two peaks and a minimum between them of  $\approx 30\%$  the peak intensity. The beam FWHM divergence is  $\sim 4.6$  mrad and the emitted laser light is unpolarized.

The Lloyd's mirror interferometer [12] scheme used in this experiment has been previously employed to print nanometer scale gratings with  $\lambda = 13$  nm radiation from a synchrotron source [2], [3]. In this wavefront division, the interferometer part of the beam impinges on the mirror at grazing incidence angle ( $\theta$ ) and is reflected to interfere with the remaining undeflected portion of the beam, as shown in Fig. 1(a). Beam interference gives rise to a sinusoidal intensity pattern of period  $d$ , defined by the wavelength of the light  $\lambda$  and the grazing incidence angle  $\theta$  according to

$$d \approx \frac{\lambda}{2 \sin(\theta)}. \quad (1)$$

Manuscript received April 26, 2005; revised July 15, 2005. This work was supported by the National Science Foundation (NSF) Engineering Research Center (ERC) for Extreme Ultraviolet Science and Technology under NSF Award EEC-0310717, by the Consejo Nacional de Investigaciones Científicas y Técnicas (CONICET), and by the W. M. Keck Foundation. The work of M. G. Capeluto was supported by CONICET under a fellowship.

M. G. Capeluto is with the Departamento de Física, Universidad de Buenos Aires, C1428EHA Buenos Aires, Argentina.

G. Vaschenko, M. Grisham, C. S. Menoni, and J. J. Rocca are with the National Science Foundation ERC for Extreme Ultraviolet Science and Technology and the Department of Electrical and Computer Engineering, Colorado State University, Fort Collins, CO 80521 USA.

M. C. Marconi is with the Departamento de Física, Universidad de Buenos Aires, C1428EHA Buenos Aires, Argentina and also with the National Science Foundation ERC for Extreme Ultraviolet Science and Technology and the Department of Electrical and Computer Engineering, Colorado State University, Fort Collins, CO 80521 USA.

S. Ludueña and L. Pietrasanta are with the Facultad de Ciencias Exactas, Centro de Microscopías Avanzadas, Universidad de Buenos Aires, C1428EHA Buenos Aires, Argentina.

Y. Lu and B. Parkinson are with the Department of Chemistry, Colorado State University, Fort Collins, CO 80521 USA.

Digital Object Identifier 10.1109/TNANO.2005.858599

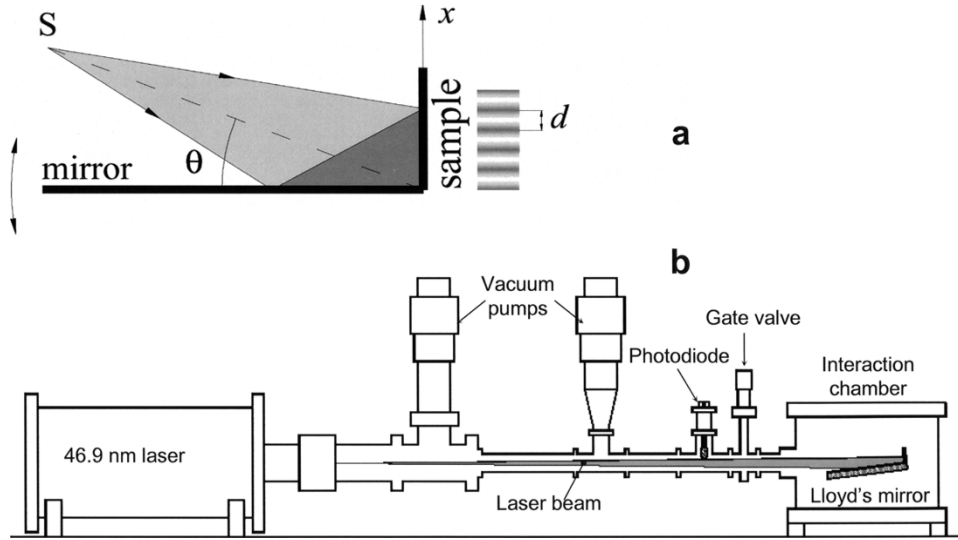


Fig. 1. (a) Schematics of the Lloyd's mirror interferometer. (b) Diagram of the nanopatterning tool implemented with the 46.9-nm laser.

Increasing the incidence angle of the incoming beam on the mirror effectively results in an increased angular separation between the two interference beams and the corresponding decrease in the interference fringe spacing. The sinusoidal intensity pattern produced by the interference has maxima and minima that are functions of the intensity of the two beams  $I_1$  and  $I_2$ , and the coherence properties of the source. Disregarding polarization effects that will be discussed later, the maximum and minimum intensities can be expressed as [12]

$$I(x) \propto I_1(x) + I_2(x) \pm 2\sqrt{I_1(x)}\sqrt{I_2(x)}|\mu_{12}(x)| \quad (2)$$

where the mutual coherence factor  $\mu_{12}$  ranging from 1 for totally coherent beams to 0 for incoherent beams is a measure of the coherence of the laser beam,  $x$  is a spatial coordinate, and the sign  $+/-$  applies for the maxima/minima in the interference pattern. The last term in (2) accounts for the intensity modulation and the corresponding fringe visibility in the interference pattern.

Strictly from wavelength considerations and according to (1), gratings with periods approaching  $\sim 24$  nm could, in principle, be printed using IL with the 46.9-nm laser. Equation (2) highlights the need for a source with a high degree of coherence, as this factor directly influences the intensity modulation term. Both the temporal and spatial coherence of the source impose limits on the printing area. For the source utilized in this experiment, the coherence radius is  $\approx 0.6$  mm at 1.8 m from the capillary exit [13],<sup>1</sup> [14]. The spatial coherence then limits the extent along the direction  $x$ , where lines can be printed to this value ( $\approx 0.6$  mm). This distance can be increased with a higher degree of spatial coherence achievable by increasing the length of the capillary plasma [11]. Considering that the bandwidth of our source is  $\lambda/\Delta\lambda \approx 10^4$ , the longitudinal coherence length is  $\approx 0.470$  mm. This parameter by itself also limits the maximum distance along  $x$  where fringes can be imprinted from 0.4 mm

to more than 6 mm for angles of incidence from  $31^\circ$  to  $2^\circ$ , as used in this experiment.

The EUV nanopatterning tool, schematically shown in Fig. 1(b), consists of the EUV laser and a 50-cm-diameter vacuum chamber where the interferometer is set up. The whole instrument is very compact and fits in an optical table within an area of  $0.7 \times 2.6$  m<sup>2</sup>. The EUV laser is connected to the interferometer chamber via a vacuum manifold that provides differential pumping of the chamber that is maintained at  $\sim 10^{-5}$  torr. The Lloyd's interferometer was constructed placing a gold-coated mirror at 1.8 m from the capillary exit at selected grazing incidence angles  $\theta$ . The mirror tilt was controlled with a vacuum compatible motorized unit. For  $2^\circ < \theta < 31^\circ$ , the interferometric fringe spacing varies from  $\sim 1300$  nm to  $\sim 45$  nm.

The sample consisted of an Si wafer spin coated with  $\sim 500$ -nm layer of PMMA (MicroChem 950 000 molecular weight). Square  $2 \times 2$  cm<sup>2</sup> pieces of the wafer were placed orthogonal to the Lloyd's mirror surface at its farthest end, as shown in Fig. 1(a). The samples were illuminated with doses consisting of typically 100 laser shots. The exposed area was defined by the laser beam FWHM diameter at the sample,  $\approx 14$  mm, and the perpendicular distance along the  $x$ -direction 0.6 mm, limited mainly by the spatial coherence. For large incidence angles ( $\theta = 31^\circ$ ), temporal coherence further reduces this distance to 0.47 mm. After exposure, the patterned PMMA was developed in a 1:3 methyl isobutyl ketone:isopropanol (MIBK:IPA) solution for  $\sim 30$  s and rinsed with abundant isopropyl alcohol and water. The resulting patterns were read using an atomic force microscope (AFM) in a tapping mode with a cantilever tip radius of 10 nm.

Fig. 2 shows the AFM images of the patterns recorded on PMMA for angles of  $15^\circ$ ,  $19^\circ$ ,  $22^\circ$ , and  $25^\circ$  corresponding to imprinted gratings of periods  $d \sim 92, 72, 63$ , and 55 nm, respectively. As can be seen, the 92-nm pattern consists of lines of well-defined edges with an average modulation depth of 12.5 nm. This relatively small modulation depth is primarily defined by the rather short absorption length of the 46.9-nm

<sup>1</sup>As in [13], we use the coherence radius  $R_c$  to define the transverse coherence of the source.  $R_c$  is defined following the convention of coherence area  $A_c = \pi R_c^2$ .

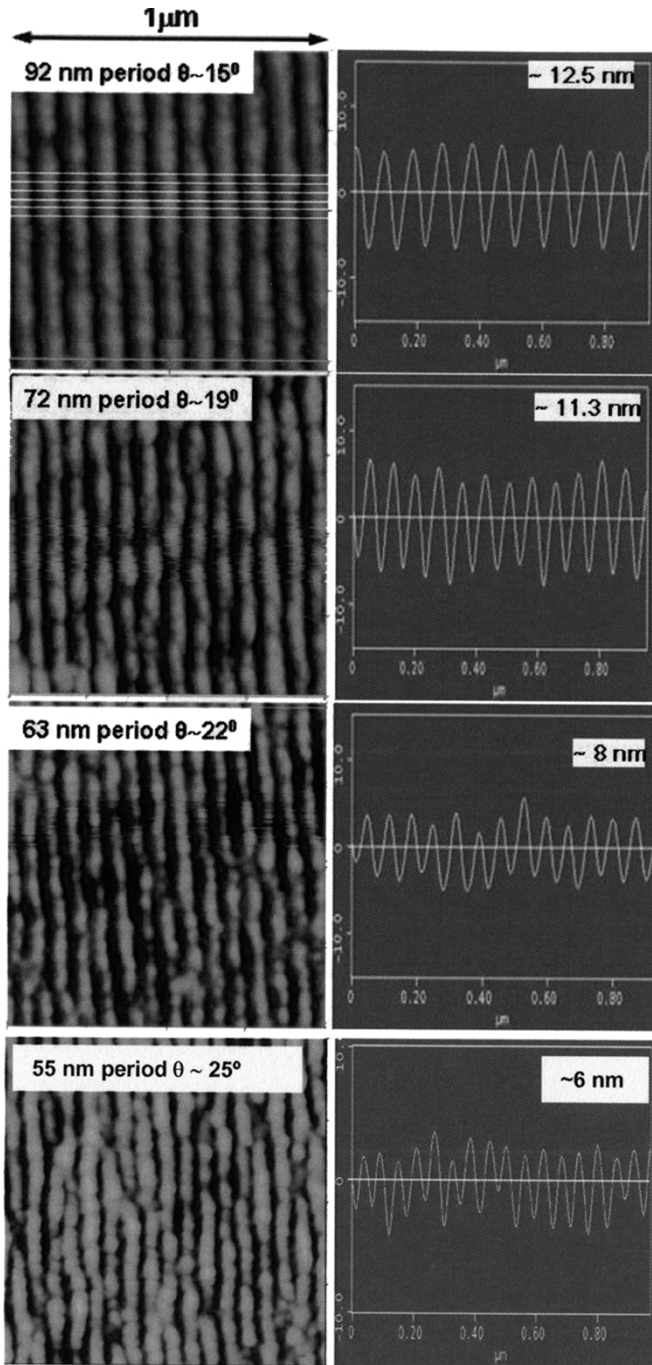


Fig. 2. (left) AFM micrographs of the grating patterns written with the 46.9-nm laser on PMMA. The angle of incidence and the grating period corresponding to each case are indicated. (right) Averaged profiles corresponding to each of the images shown above. The average modulation depths are indicated in the top right corners.

light in PMMA, which is approximately 20 nm.<sup>2</sup> Utilizing recently developed high repetition rate table-top lasers at shorter wavelengths (18.9–13.2 nm) [15]–[17], the modulation depth can be significantly increased; as for these wavelengths, the expected penetration depth is  $\approx 200$  nm [18]. For smaller line periods ( $< 60$  nm), the modulation depth decreases and the line edge roughness is observed to increase significantly.

<sup>2</sup>[Online]. Available <http://www-cxro.lbl.gov/>

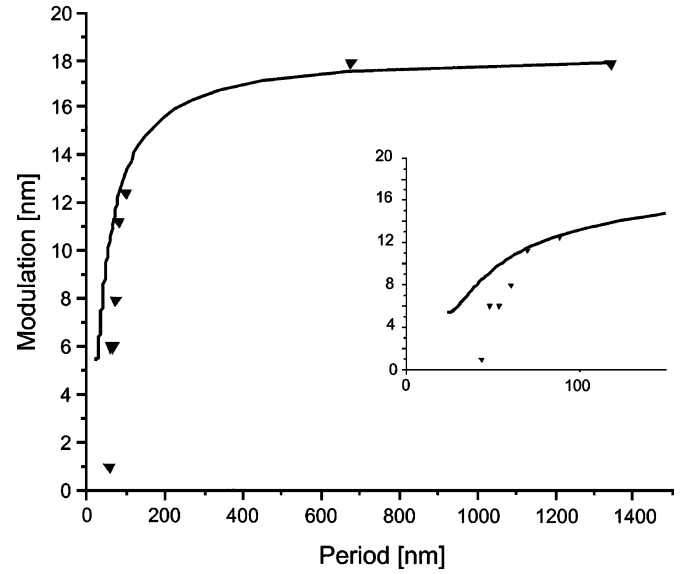


Fig. 3. Calculated (solid line) and measured modulation depth (triangles) of the gratings on PMMA surface shown as a function of the grating period. The insert is a blow-up of the data for periods smaller than 150 nm.

On the assumption that the modulation depth is proportional to the difference between the maximum and minimum intensities in the interference pattern, as the light is completely absorbed in the PMMA, the reduction in the modulation depth with the decrease of the line period can be accounted for by two dominant effects. One is the decrease in the mirror reflectivity for increased grazing angles. The other factor arises from the dependence of the fringe visibility corresponding to the TM component of the unpolarized reflected beam on the angle of incidence [19]. For this polarization, the fringe visibility approaches zero as the angle between the two beams approaches  $90^\circ$ . For the other polarization (TE), both electric field vectors are always parallel to each other independent of the incidence angle [19]. To compute the total unpolarized intensity incident on the sample, we expressed the reflected portion of the beam as  $I_2 = R(\theta)I_1$  and calculated the intensity  $I$  of the interfering beams as a superposition of the TM and TE polarizations in equal parts as follows:

$$I = \frac{1}{2} \left( I_1 + R^{\text{TE}} I_1 \pm 2I_1 \sqrt{R^{\text{TE}}} \right) + \frac{1}{2} \left[ I_1 + R^{\text{TM}} I_1 \pm 2I_1 \sqrt{R^{\text{TM}}} \cos(2\theta) \right]. \quad (3)$$

In (3),  $R^{\text{TE}}$  and  $R^{\text{TM}}$  are the gold mirror reflectivities for each polarization,<sup>3</sup> and  $2\theta$  is the angle between the two beams at the sample. The  $+/-$  sign has the same meaning as in (2).

Fig. 3 compares the measured modulation depth of the imprinted gratings with the computed difference between intensity maxima and minima as a function of the grating period calculated using (3). In this graph, the calculated modulation depth was normalized to the maximum experimental value equal to 18 nm at the angle  $\theta = 2^\circ$ . This figure shows that the measured modulation depth follows the general trend of the calculated values, thus confirming the dominant role of the interfer-

<sup>3</sup>[Online]. Available: <http://cletus.phys.columbia.edu/~windt/idl/imd/>

ence fringe visibility in defining the modulation depth. A more detailed comparison (insert in Fig. 3) shows, however, a deviation between the calculation and experiment at very small periods ( $\leq 55$  nm). Several factors not considered in our computations can also play a role in degrading the modulation depth of the PMMA gratings. Among them are the contributions of mechanical vibrations during exposure, scattering due to the mirror's roughness that further reduces the intensity of the reflected beam, the size of the AFM probe tip that is comparable to the smallest periods, and possibly the limits of the resolution of the photoresist.

In summary, we have realized the first demonstration of nanometer-scale patterning using a table-top EUV laser. Dense line patterns with a period as small as 55 nm were imprinted in PMMA using a 46.9-nm laser and Lloyd's mirror interferometer. Improved aspect ratio in the periodic nanopatterning could be expected with the utilization of recently demonstrated high repetition rate shorter wavelength lasers due to the larger penetration depth in the photoresist. These results show that EUV lasers have the potential of becoming a useful tool for printing nanometer features for selected applications.

## REFERENCES

- [1] V. N. Golovkina, P. F. Nealey, F. Cerrina, J. W. Taylor, H. H. Solak, C. David, and J. Gobrecht, "Exploring the ultimate resolution of positive-tone chemically amplified resists: 26 nm dense lines using extreme ultraviolet interference lithography," *J. Vac. Sci. Technol. B, Microelectron. Process. Phenom.*, vol. 22, pp. 99–103, 2004.
- [2] H. H. Solak, D. He, W. Li, S. S. Gasson, S. S. Cerrina, B. H. Sohn, X. M. Yang, and P. Nealey, "Exposure of 38 nm period grating patterns with extreme ultraviolet interferometric lithography," *Appl. Phys. Lett.*, vol. 75, pp. 2328–2330, 1999.
- [3] H. H. Solak, D. He, W. Li, and F. Cerrina, "Nanolithography using extreme ultraviolet lithography interferometry: 19 nm lines and spaces," *J. Vac. Sci. Technol. B, Microelectron. Process. Phenom.*, vol. 17, pp. 3052–3057, 1999.
- [4] S. H. Zaidi and S. R. J. Brueck, "Multiple-exposure interferometric lithography," *J. Vac. Sci. Technol. B, Microelectron. Process. Phenom.*, vol. 11, pp. 658–666, 1993.
- [5] Z. Yu, W. Wu, L. Chen, and S. Chou, "Fabrication of large area 100 nm pitch grating by spatial frequency doubling and nanoimprint lithography for subwavelength optical applications," *J. Vac. Sci. Technol. B, Microelectron. Process. Phenom.*, vol. 19, pp. 2816–2819, 2001.
- [6] T. A. Savas, S. N. Shah, M. L. Schattenburg, J. M. Carter, and H. I. Smith, "Achromatic interferometric lithography for 100-nm-period gratings and grids," *J. Vac. Sci. Technol. B, Microelectron. Process. Phenom.*, vol. 13, pp. 2732–2735, 1995.
- [7] M. Switkes, T. M. Bloomstein, and M. Rothschild, "Patterning of sub-50 nm dense features with space-invariant 157 nm interference lithography," *Appl. Phys. Lett.*, vol. 77, pp. 3149–3151, 2000.
- [8] W. Hinsberg, F. A. Houle, J. Hoffnagle, M. Sanchez, G. Wallraff, M. Morrison, and S. Frank, "Deep-ultraviolet interferometric lithography as a tool for assessment of chemically amplified photoresist performance," *J. Vac. Sci. Technol. B, Microelectron. Process. Phenom.*, vol. 16, pp. 3689–3694, 1998.
- [9] A. Yen, E. Anderson, R. A. Ghanbari, M. Schattenburg, and H. Smith, "Achromatic holographic configuration for 100-nm-period lithography," *Appl. Opt.*, vol. 31, pp. 4540–4545, 1992.
- [10] B. Benware, C. Moreno, D. Burd, and J. J. Rocca, "Operation and output pulse characteristics of an extremely compact capillary-discharge tabletop soft-X-ray laser," *Opt. Lett.*, vol. 22, pp. 796–798, 1997.
- [11] C. D. Macchietto, B. R. Benware, and J. J. Rocca, "Generation of millijoule-level soft-X-ray laser pulses at a 4-Hz repetition rate in a highly saturated tabletop capillary discharge amplifier," *Opt. Lett.*, vol. 24, pp. 1115–1117, 1999.
- [12] M. Born and E. Wolf, *Principles of Optics*, 7th ed. Cambridge, U.K.: Cambridge Univ. Press, 1999.
- [13] J. W. Goodman, *Statistical Optics*. New York: Wiley, 1985, pp. 171–187.
- [14] Y. Liu, M. Seminario, F. G. Tomasel, C. Chang, J. J. Rocca, and D. T. Attwood, "Achievement of essentially full spatial coherence in a high-average-power soft-X-ray laser," *Phys. Rev. A, Gen. Phys.*, vol. 63, 2001, Art. 033 802.
- [15] B. M. Luther, Y. Wang, M. A. Larotonda, D. Alessi, M. Berrill, M. C. Marconi, J. J. Rocca, and V. N. Shlyaptsev, "Saturated high-repetition-rate 18.9-nm tabletop laser in nickellike molybdenum," *Opt. Lett.*, vol. 30, pp. 165–167, 2005.
- [16] Y. Wang, M. A. Larotonda, B. M. Luther, D. Alessi, M. Berril, V. N. Shlyaptsev, and J. J. Rocca, "Demonstration of high repetition rate tabletop soft X-ray lasers with saturated output at wavelengths down to 13.9 nm and gain down to 10.9 nm," *Phys. Rev. Lett.*, submitted for publication.
- [17] R. Keenan, J. Dunn, P. K. Patel, D. F. Price, R. F. Smith, and V. N. Shlyaptsev, "High-repetition-rate grazing-incidence pumped X-ray laser operating at 18.9 nm," *Phys. Rev. Lett.*, vol. 94, 2005, Art. 103 901.
- [18] C. Jacobsen and M. Howells, "A Technique For projection X-ray lithography using computer generated holograms," *J. Appl. Phys.*, vol. 71, pp. 2993–3001, 1992.
- [19] A. Biswas and S. R. J. Brueck, "Simulation of the 45-nm half-pitch node with 193-nm immersion lithography—Imaging interferometric lithography and dipole illumination," *J. Microlith., Microfab., Microsyst.*, vol. 3, pp. 35–43, 2004.



**Maria G. Capeluto** was born in Buenos Aires, Argentina, in 1977. She received the Licenciado Diploma degree in physics from the Universidad de Buenos Aires, Buenos Aires, Argentina, in 2002, and is currently working toward the Ph.D. degree at the Universidad de Buenos Aires. Her doctoral research concerns new approaches to nanopatterning.

She is a visiting graduate student with the National Science Foundation (NSF) Engineering Research Center for EUV Science and Technology, Colorado State University, Fort Collins. Her research interests

include two photon absorption fluorescence microscopy and the development of nanopatterning techniques using table-top EUV lasers.



**Georgiy Vaschenko** was born in Moscow, Russia, in 1966. He received the Ph.D. degree in electrical engineering from Colorado State University, Fort Collins, in 2002.

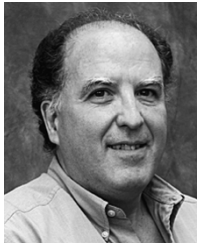
He is currently with the National Science Foundation (NSF) Engineering Research Center for EUV Science and Technology, Colorado State University, Fort Collins. His research interests include interaction of EUV emission with matter, high-resolution EUV microscopy, ultrafast optical diagnostic techniques, and optics of semiconductor

materials and devices.



**Michael Grisham** received the B.S. degree in electrical and computer engineering from Colorado State University, Fort Collins, in 2002, and is currently working toward the M.S. degree (with interests in the engineering of EUV laser sources and their applications) at Colorado State University.

He is a key contributor to recent studies of imaging, patterning, and laser ablation with short-wavelength sources.



**Mario C. Marconi** is currently a Professor with the Electrical and Computer Engineering Department, Colorado State University, Fort Collins. As a participating faculty member with the National Science Foundation (NSF) Engineering Research Center for EUV Science and Technology, Colorado State University, his interests include the development of table-top EUV lasers and the applications of EUV coherent sources in metrology and nanotechnology.

Dr. Marconi is a member of the Optical Society of America (OSA) and the Argentinean Physical Society.



**Bruce Parkinson** received the B.S. degree in chemistry from Iowa State University, Ames, in 1972, and the Ph.D. degree from the California Institute of Technology, Pasadena, in 1977.

Following a year of post-doctoral studies with Bell Laboratories, he became a Staff Scientist with the Ames Laboratory. In 1981, he joined the Solar Energy Research Institute, Golden, CO, as a Senior Scientist. In 1985, he joined the Central Research and Development Department, DuPont Company, where he remained until he became a Professor of chemistry with Colorado State University, Fort Collins, in 1991. His research covers a wide range of areas including materials chemistry, surface chemistry, and photoelectrochemistry.

**S. Ludueña**, photograph and biography not available at time of publication.

**L. Pietrasanta**, photograph and biography not available at time of publication.



**Yunfeng Lu** received the Bachelor's degree from JiLin University, Changchun, China, in 1999, and is currently working toward the Ph.D. degree in chemistry at Colorado State University, Fort Collins.

His research interests involve photo-electrochemistry and scanning probe microscopy.



**Carmen S. Menoni** (SM'99) is currently a Professor of electrical and computer engineering with Colorado State University, Fort Collins. As a member of the National Science Foundation (NSF) Engineering Research Center for EUV Science and Technology, Colorado State University, her group is engaged in the demonstration of high-resolution imaging and patterning schemes with EUV lasers. Other aspects of her research include the study of the ultrafast dynamics of semiconductor lasers and related heterostructure materials. She is an Editorial Board member of the *Review of Scientific Instruments*.

Prof. Menoni is a member of the American Physical Society and Optical Society of America (OPS). She is an associate editor for the IEEE JOURNAL OF QUANTUM ELECTRONICS. She co-chaired The International Society for Optical Engineers (SPIE) Symposium on Semiconductor Lasers for Lightwave Communications at ITCOM'01 and ITCOM'02 and has been member of the Optical Materials, Fabrication, and Characterization Committee Conference on Lasers and Electro-Optics.

**J. J. Rocca**, photograph and biography not available at time of publication.